ELSEVIER

Thermochimica Acta 267 (1995) 29–44

thermochimica acta

# Thermal analysis and kinetics of solid state reactions[1]

Haruhiko Tanaka

*Chemistry Laboratory, Faculty of School Education, Hiroshima University, 1-1-1 Kagamiyama, Higashi-Hiroshima, 739, Japan*

Received 30 November 1994; accepted 17 March 1995

**Abstract**

Some early studies of the rate of solid-state reactions are briefly reviewed in connection with the later development of techniques for determining kinetic parameters under non-isothermal conditions. The fundamental kinetic equations for the non-isothermal reactions are reexamined in an attempt to increase the reliability of the kinetic parameters obtained for solid state reactions. It is suggested that reliable kinetic parameters are obtained in terms of kinetic equations with non-integral kinetic exponents. The significance of such a kinetic approach as well as the usefulness of the reduced time are discussed and illustrated by the kinetic analysis of several decompositions of solids. It is stressed that the isoconversion methods, isothermal or non-isothermal, are quite appropriate for obtaining reliable kinetic parameters and in turn for understanding the kinetics of solid state reactions in a comprehensive and sophisticated way.

*Keywords:* TA; Kinetics; Solid state reaction

## 1. Introduction

The thermobalance invented by K. Honda in 1915 is worth noting in that thermogravimetry (TG) stimulated studies of the rate of solid state reactions such as thermal decomposition of solid materials [1]. One pioneering work on the kinetics of solid state decomposition appeared in 1925, in which a theoretical approach and the analysis of mass loss of insulating materials, e.g. cotton, paper, and silk are made by TG at constant temperatures, using the following equation [2]:

[1] Presented at the 30th Anniversary Conference of the Japan Society of Calorimetry and Thermal Analysis, Osaka, Japan, 31 October–2 November 1994.


*SSDI* 0040-6031 (95) 02464-6

$$\log(t) = \frac{Q}{T} - f(m) \tag{1}$$

where $t$, $Q$, $T$ and $f(m)$ are the time, a constant depending on the material, the absolute temperature, and a function of the ratio of mass loss $m$, respectively. In 1928, Akahira analyzed the kinetics of deterioration of cotton under the condition of temperature change [3]. He introduced a fundamental derivative kinetic equation which is applicable to reactions under both isothermal and non-isothermal conditions.

$$\frac{dm}{dt} = C\exp(-Q/T)f'(m) \tag{2}$$

where $C$ and $f'(m)$ are a constant and another function of $m$, respectively. He also defined the equivalent temperature, $T_e$, for a regular cyclic temperature change.

$$T_e = \frac{Q}{\log\{[\int_0^\tau \exp(-Q/T)\,dt]/\tau\}} \tag{3}$$

where $\tau$ is the period of a cycle and $T$ is a function of time. It was shown that at $T_e$ the rate of deterioration is equal to that subjected to the cycle. He also published a numerical table of exponential integral functions, which can be used in calculating the integral in the equivalent temperature for constant rate heating and cooling as well as for exponential heating and cooling [4]. Doyle published a similar table later in 1961 which has been widely used in obtaining the integral values often required for analyzing the kinetics of non-isothermal solid state reactions [5].

Although DTA was also used in analyzing the kinetics of solid state reactions, which are not accompanied by a mass change in the sample, the reliability in general is inferior to that from TG. In particular, it is relatively difficult to accurately determine the fractional reaction as a function of time or temperature from DTA. In addition, there are other normal factors which lead to reduction of the reliability of kinetic parameters obtained by thermal analysis, e.g. non-stationary distribution of temperature, non-linear temperature increase of the sample and so on. DSC, which was invented in 1963, made it possible to accurately analyze the kinetics of solid state reactions, in which no mass change in the sample necessarily occurs. Such a technique for kinetic analysis by use of DSC has several advantages over that by use of TG or DTA, although the maximum temperature available for DSC is lower than that of DTA.

The work by Kujirai-Akahira [2] and Akahira [3] gave the very basis for isoconversion methods of kinetic analysis of thermoanalytical data. We can classify the isoconversion methods so far developed for non-isothermal kinetics into three types: (1) the Flynn–Wall–Ozawa (FWO) method; (2) the Kissinger–Akahira–Sunose (KAS) method; and (3) the Expanded Friedman method [6]. Although a great number of methods of kinetic analysis of non-isothermal solid state reactions other than the three methods above have been proposed and used, here we are concerned with these three isoconversion methods, which are considered to be most reliable.

## 2. Kinetic equations

### 2.1. Derivation of expressions for isoconversion methods

By using the reduced time $\theta$ introduced by Ozawa [7], the fundamental equation is assumed as follows [6]:

$$\theta = \int_0^t \exp(-E/RT)\,\mathrm{d}t \tag{4}$$

$$\alpha = \varphi(\theta) \tag{5}$$

where $E$, $R$, $\alpha$, and $\varphi(\theta)$ are the activation energy, the gas constant, the fractional reaction, and an eigen-valued function of $\theta$, respectively. We also assume that the Arrhenius law is applicable to the solid state reactions.

$$k = A\exp(-E/RT) \tag{6}$$

where $k$ and $A$ are the rate constant and the preexponential factor, respectively. If the reaction proceeds through a single elementary process, $\varphi(\theta)$ is constant at a given fractional reaction $\alpha$. $\theta$ is given by the following equation at a constant heating rate $\phi$, neglecting the conversion rate at a low temperature.

$$\theta = \frac{E}{\phi R}\, p\left(\frac{E}{RT}\right) \tag{7}$$

where $p$ is the function given by Doyle [5].

By using the approximation of $\log p(y) = -2.315 - 0.4567y$ $(20 < y < 60)$, the equation of the FWO method is obtained [7–9].

$$\log\phi + 0.4567\frac{E}{RT} = \text{constant} \tag{8}$$

If the approximation of $p(y) = \exp(-y)/y^2$ $(20 < y < 50)$ is applied, the following expression for the KAS method can be derived [9–11].

$$\ln\frac{\phi}{T^2} + \frac{E}{RT} = \text{constant} \tag{9}$$

The activation energy $E$ is obtained by plotting $\log\phi$ or $\ln(\phi/T^2)$ against $1/T$ based on Eq. (8) or (9), respectively.

By differentiating Eq.(5), we obtain

$$\frac{\mathrm{d}\alpha}{\mathrm{d}\theta} = \varphi'(\theta) \tag{10}$$

At a given fractional conversion $\alpha$, $d\alpha/d\theta$ is constant.

$$\frac{d\alpha}{d\theta} = \frac{d\alpha}{dt}\frac{dt}{d\theta} = \frac{d\alpha}{dt}\exp\left(\frac{E}{RT}\right) = \text{constant} \tag{11}$$

The following relationship is then obtained:

$$\frac{d\alpha}{dt} \propto \exp\left(-\frac{E}{RT}\right) \tag{12}$$

Therefore, a plot of $\ln(d\alpha/dt)$ versus $1/T$ gives a linear relationship, from which the $E$ value can be determined. It is important to note that Eq. (12) can be applied to any TA data obtained under any condition of temperature change, because the equation derived for the so-called Expanded Friedman methods holds for any temperature change [12,13]. It is a great advantage that this method is successfully applied to a TA curve even if the programmed temperature condition was distorted by the self-cooling or self-heating during the reaction.

For isothermal analyses of the kinetics of solid state reactions, the following fundamental differential kinetic equation is used:

$$\frac{d\alpha}{dt} = kf(\alpha) \tag{13}$$

Alternatively, an integral type of equation is used:

$$g(\alpha) = kt, \quad \text{with } g(\alpha) = \int_0^\alpha \frac{1}{f(\alpha)}\,d\alpha \tag{14}$$

An appropriate kinetic model function $g(\alpha)$ is usually estimated by plotting $g(\alpha)$ versus $t$, based on Eq. (14). The rate constant $k$ is also evaluated from the slope of the line obtained. Normally the activation energy $E$ and the preexponential factor $A$ are determined using the $k$ values obtained at different temperatures. Such values are averaged over the whole extent of the reaction.

It is often useful to obtain the $E$ value at a given fractional conversion. The following equations, integral and differential, are easily derived from Eqs. (6), (13) and (14).

$$-\ln t = -\frac{E}{RT} + \ln\left[\frac{A}{g(\alpha)}\right] \tag{15}$$

$$\ln\left(\frac{d\alpha}{dt}\right) = -\frac{E}{RT} + \ln[Af(\alpha)] \tag{16}$$

### 2.2. Kinetic model functions

Normally several basic functions that were derived by assuming simply idealized models are used for the kinetic study of the solid state reactions. Table 1 summarizes such functions, in which the exponents are integers except $m$ in the $A_m$ functions. In practice, however, the disagreement between the idealized process assumed in formulating the kinetic functions and the actual process under investigation has to be taken into account, because this disagreement leads to some distortion of the Arrhenius parameters. To avoid such a distortion, an empirical function $h(\alpha)$ of the Sestak-Berggren (SB) model can be used [14,15]. In terms of $h(\alpha)$, the apparent but characteristic Arrhenius parameters can be obtained from the TA curves. Introducing the accommodation function $a(\alpha)$, the SB model is regarded as the function accommodating the distortion of the actual process from the idealized model. It is very difficult, however, to formalize, based on the real physicochemical aspect, and can be expressed by the empirical (analytical) formula [16].

#### 2.2.1. Contracting geometry type reactions

The equation of the contracting volume controlled by chemical reaction, the $R_3$ law, for example, is derived by assuming an isotropic shrinkage of a cubic or spherical reactant particle with a constant rate of interface advancement. As will be seen later, however, the reactant particle is normally far from cubic or spherical and the reactivity of the reaction front often shows anisotropy depending on the crystallographic direction of the reactant and/or product. From polarizing microscopic observation of an internal surface

Table 1

Kinetic model functions $f(\alpha)$ usually employed for the solid state reactions, together with those integral forms $g(\alpha)$

| Model | Symbol | $f(\alpha)$ | $g(\alpha)=\int_0^\alpha \frac{d\alpha}{f(\alpha)}$ |
|---|---|---|---|
| One-dimensional diffusion | $D_1$ | $\frac{1}{2\alpha}$ | $\alpha^2$ |
| Two-dimensional diffusion | $D_2$ | $-\frac{1}{\ln(1-\alpha)}$ | $\alpha+(1-\alpha)\ln(1-\alpha)$ |
| Three-dimensional diffusion (Jander) | $D_3$ | $\frac{3(1-\alpha)^{2/3}}{2[1-(1-\alpha)^{1/3}]}$ | $[1-(1-\alpha)^{1/3}]^2$ |
| Three- dimensional diffusion (Ginstring-Brounshtein) | $D_4$ | $\frac{3}{2[(1-\alpha)^{-1/3}-1]}$ | $1-\frac{2\alpha}{3}-(1-\alpha)^{2/3}$ |
| Phase boundary controlled | $R_n$ $(1\le n\le 3)$ | $n(1-\alpha)^{1-1/n}$ | $1-(1-\alpha)^{1/n}$ |
| Nucleation and growth (Avrami-Erofeev) | $A_m$ $(0.5\le m\le 4)$ | $m(1-\alpha)[-\ln(1-\alpha)]^{1-1/m}$ | $[-\ln(1-\alpha)]^{1/m}$ |

of partially dehydrated single crystals of lithium sulfate monohydrate, it was found that both flat and wavy fronts result on the reaction fronts advancing inwards [17]. This difference in the reaction fronts seems to arise from changes in the nucleation density on the corresponding original surface and in the degree of stress and/or strain at the phase boundary, depending on the crystallographic direction. This in turn leads to different reactivities at the reaction interfaces and thus to different rate behaviors. It is likely that the reaction geometry of the overall reaction cannot be expressed in terms of an integral value of $n$. A non-integral value $N$ instead of the integral value $n$ can be used to accommodate the distortion of the actual reaction geometry from the idealized one [18]. Regarding the $R_n$ law with $n = 1$ and 2, a similar treatment is possible. Therefore, the following function can be used instead of the $R_n$ function:

$$R_N = N(1-\alpha)^{1-1/N}, \quad \text{with } 1 < N < 3 \tag{17}$$

It is interesting that the non-integral value of $N$ is taken as the value corresponding to the fractal dimension $Q$, although the relationship between $N$ and $Q$ varies due to the macroscopic character of TA curves. However, the Arrhenius parameters obtained seem to be characteristic of the process under the conditions investigated, because the distortion of the Arrhenius parameters by an inappropriate $f(\alpha)$ with an integral dimension was reduced by applying the non-integral exponent $N$, which is thought to be reasonable for the complex reaction geometry observed microscopically [18].

*2.2.2. Contracting geometry controlled by diffusion*

Using similar considerations, the kinetic model functions of contracting geometry controlled by diffusion, i.e. the $D_1$, $D_2$, $D_3$ and $D_4$ laws can be extended to those with non-integral exponents $Q$. Ozao and Ochiai derived the following functions, based on the fractal nature of pulverized solid particles [19]:

$$F(\alpha) = \frac{1}{1-(1-\alpha)^{2/Q-1}}, \quad \text{with } 1 \le Q < 2 \tag{18}$$

$$F(\alpha) = \frac{1}{(1-\alpha)^{2/Q-1}-1}, \quad \text{with } 2 < Q \le 3 \tag{19}$$

When $Q = 1$ and 3, Eqs. (18) and (19) correspond to the $D_1$ and $D_4$ laws, respectively. It is likely that in the reaction yielding a gaseous product the rate of interface advancement changes during the course of the reaction, affected by the self-generated reaction condition at the reaction interface. In such a case, the condition of constant rate of advancement of the reaction interface assumed for the $R_n$ model can no longer be fulfilled. It is reasonable here to assume that the rate behavior of interface advancement is described by the $p$th order law [18]. Considering the reaction geometry, we obtain

$$F(\alpha) = \frac{n(1-\alpha)^{1-1/n}}{p[1-(1-\alpha)^{1/n}]^{p-1}} \tag{20}$$

When $p = 1$ and 2 for $n = 3$, Eq. (20) corresponds to the $R_3$ and $D_3$ laws, respectively. With $p = 2$ and $n = N$, Eq. (20) is regarded as the fractal description of the $D_3$ law.

*2.2.3. Nucleation and growth type equations*

The Avarami-Erofeyev equation is derived by assuming the following topokinetic features [20]:

(1) the existence of a potential site for nucleation;
(2) the nucleation rate can be expressed by a constant or linear law;
(3) the nuclei grow isotropically;
(4) the rate of advancement of the reaction interface is controlled by either chemical reaction, i.e. the linear law or diffusion, i.e., the parabolic law;
(5) the reaction interface is simple reactant-product contact and the rate equation of interface advancement does not change during the course of reaction.

The integral exponent $m$ in the differential $A_m$ functions is given by

$$m = \beta + \frac{\lambda}{\chi} \tag{21}$$

where $\beta$, $\lambda$ and $\chi$ are the kinetic exponents of the rate equation for nucleation (0 or 1), of the growth dimension (1, 2, or 3) and of the rate equations for interface advancement (1 or 2), respectively. In the actual process, non-integral exponents can be introduced, as is the case with the contracting geometry model, because the conditions (2)–(5) are thought not to be met. Accordingly, the $A_m$ law is replaced by the $A_M$ law, in which $M$ refers to non-integral values. These kinetic model functions with the non-integral exponents can be considered as a distorted case of the conventional $f(\alpha)$. This can be expressed by the product of $f(\alpha)$ with integral exponents and the accommodation function. Alternatively, the non-integral exponents $M$ can be taken as those corresponding to the fractal dimension.

Once the activation energy has been determined, we can find the kinetic law which best describes a measured set of TA data. Introducing the reduced time $\theta$ into the kinetic analysis, the useful expression for selecting an appropriate $G(\alpha)$ function is derived [7,9].

$$G(\alpha) = A\theta \tag{22}$$

where $\theta$ is given by Eq. (7). When a differential function $F(\alpha)$ is used instead of the integrated function $G(\alpha)$, we obtain [16,21]

$$y(\alpha) = \frac{d\alpha}{d\theta} = AF(\alpha) \tag{23}$$

$y(\alpha)$ can be calculated using Eq. (11). Therefore, either a plot of $G(\alpha)$ versus $\theta$ or $d\alpha/d\theta$ versus $F(\alpha)$ yields a straight line with a slope of $A$, if an appropriate $G(\alpha)$ or $F(\alpha)$ is used. It is also possible to estimate an appropriate kinetic model function by considering that the $z(\alpha)$ function, which is defined as $z(\alpha) = F(\alpha)G(\alpha)$, has maxima at $\alpha_p^\infty$ for the kinetic models except $D_1$ and $R_1$, listed in Table 1. $\alpha_p^\infty$ stands for $\alpha_p$, which corresponds to the

Table 2
The values of $\alpha_p^\infty$ which yield the maximum of the $z(\alpha)$ function

| Model | $A_m$ | $R_2$ | $R_3$ | $D_2$ | $D_3$ | $D_4$ |
|---|---|---|---|---|---|---|
| $\alpha_p^\infty$ | 0.632 | 0.750 | 0.704 | 0.834 | 0.704 | 0.776 |

fractional reaction at the maximum of the TA peak, when $x_p$ ( = $E/RT_p$) is infinite [16,21]. Table 2 shows the characteristic values of $\alpha_p^\infty$ for the kinetic model functions.

## 3. Kinetic analysis of some solid state reactions

### *3.1. Potassium copper(II) chloride dihydrate $K_2CuCl_4 \cdot 2H_2O$ [22]*

It is interesting that the non-isothermal dehydration of single crystals of this dihydrate proceeds in three distinct stages, but the crushed crystals are dehydrated in a single step under similar experimental conditions to the dehydration of single crystals. It seems that the simpler dehydration behavior of crushed crystals, compared with that of the single crystal material is explained by (1) the decreased influence of the vapor pressure of self-generated water and less blocking action by the solid product layer and (2) the fact that the TA curves for the dehydration of the former are based on average over a great number of particles, whereas that of the latter is specific to the material with anisotropy.

By plotting $G(\alpha)$ versus $\theta$ based on Eq. (22), the $R_N$ laws were estimated as appropriate. The activation energy was determined by using the KAS method. These results were comparable with those obtained isothermally.

### *3.2. Lithium sulfate monohydrate $Li_2SO_4 \cdot H_2O$ [17,23,24]*

It was found from plots of $G(\alpha)$ versus $\theta$ that the overall kinetics of non-isothermal dehydration of single-crystals and crushed crystals of the monohydrate obeys the rate equation, $R_N = A\theta$ with $2 < N < 3$. The kinetics of isothermal dehydration of this monohydrate was described by the similar rate equation, $R_N = kt$ with a little different $N$ value from the non-isothermal dehydration. The kinetic obedience of the $R_N$ law was verified by microscopic observation, in polarizing light, of thin sections of single crystal materials dehydrated to different fractional reactions [24]. It was also noted that the reaction front is not single sharp discontinuity showing anisotropy (see Fig. 1).

The activation energies $E$ for the thermal dehydration of the crushed crystals of lithium sulfate monohydrate (100–170 mesh) were determined based on the TG and DTG curves in terms of Eqs. (9), (12), (15) and (16). Fig. 2 shows the activation energies $E$ determined from the four different isoconversion methods [25]. We see that the values $E$ are different not only between the isothermal and non-isothermal measurements, but also between the integral and differential methods of kinetic evaluation. Although it is generally acceptable that differential methods of kinetic calculation are more suitable in obtaining meaningful kinetic parameters than integral methods, it is evident that this de-

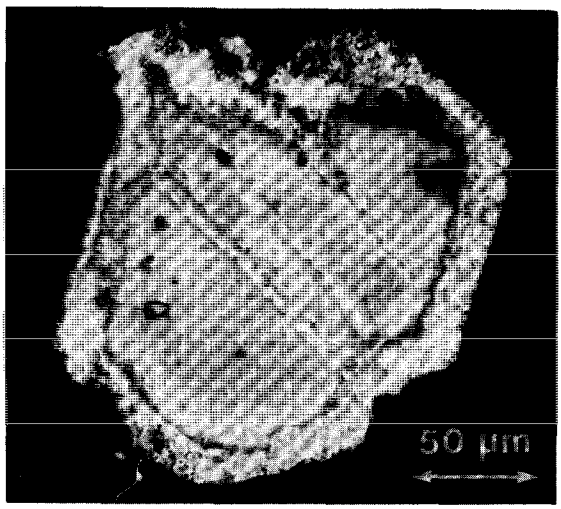


Fig. 1. A typical microscopic view of the internal surface of a 50% dehydrated crushed crystal of $Li_2SO_4 \cdot H_2O$ of −48 + 100 mesh sieve fraction (from Fig. 2 in Ref. [24]; reproduced by permission of Elsevier).

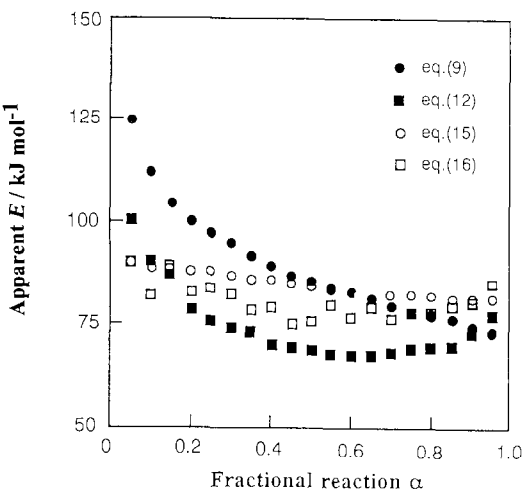


Fig. 2. Comparison of the apparent activation energies $E$ determined, in terms of four different equations, from TG curves for the isothermal and non-isothermal dehydrations of crushed crystals of $Li_2SO_4 \cdot H_2O$ (−100 + 170 mesh) in $N_2$ flow.

pends on the reliability of the TA curves from the kinetic point of view. As stated above, the reliability varies depending on the degree of deviation in the actual reaction condition from that predetermined or idealized from the reaction itself. This also depends on the kind of TA technique, the design of the equipment, the experimental conditions and the nature of the reaction under investigation.

### 3.3. Copper(II) acetate monohydrate $Cu(CH_3COO)_2 \cdot H_2O$ [26]

Plots of $g(\alpha)$ and/or $G(\alpha)$ versus $\theta$ showed that the kinetics of non-isothermal dehydration of single crystals of this monohydrate is described by a three-dimensional diffusion controlled law (the Jander law), $D_3 = A\theta$, although the contracting geometry law was not markedly inferior. The obedience of the Jander law was more marked at higher heating rates and in the later stage of the reaction. It was found, on the other hand, that the isothermal dehydration is controlled by a contracting geometry law, $R_N = kt$, with $2 < N < 3$. This was evidenced by polarizing microscopic observation of internal surfaces of the partially dehydrated single crystals. It was deduced that a wavy reaction front proceeds along the direction of cleavage (the $c$-axis). An optically different layer, which is evidence of a strain zone of appreciable thickness (ca. 30 $\mu$m), was recognized on the reactant side adjacent to the reaction front.

The activation energies $E$ and the preexponential factors $A$ obtained isothermally were a little larger than those determined from the KAS method of analysis of the non-isothermal process. These kinetic parameters were mutually correlated by the following equation:

$$\ln A = a + bE, \quad \text{with } b > 0 \tag{24}$$

where $a$ and $b$ are constants. Eq. (24) implies that any increase of the activation energy $E$ is accompanied by an increase of the preexponential factor $A$, i.e. the two parameters vary in parallel to keep the rate constant $k$ nearly unchanged for a given solid state reaction. Such a relationship is often called the kinetic compensation effect (KCE), which was originally found for heterogeneous catalytic reactions [16,25,27].

### 3.4. Synthetic malachite $Cu_2CO_3(OH)_2$ [28,29]

Synthetic malachite decomposes thermally in a single step as follows [28]:

$$Cu_2CO_3(OH)_2 \rightarrow 2CuO + CO_2 + H_2O$$

Fig. 3 shows typical TG curves for the thermal decomposition of synthetic malachite with a sample size of 10.0 mg at various heating rates from 1 to 10 K min$^{-1}$ at a reduced pressure of $-1.5 \times 10^{-2}$ Pa. The TG curves were kinetically analyzed by use of the Expanded Friedman method and the activation energy $E$ was determined to be 131 kJ mol$^{-1}$ in the range $0.20 < \alpha < 0.95$. By using this value, $d\alpha/d\theta$ was calculated to find the $\alpha_M$ which refers to the $\alpha$ value where $d\alpha/d\theta$ reaches the maximum. The appropriate kinetic function was then estimated as the $A_M$ or SB($m$,$n$) function. By assuming the $A_M$ law, a

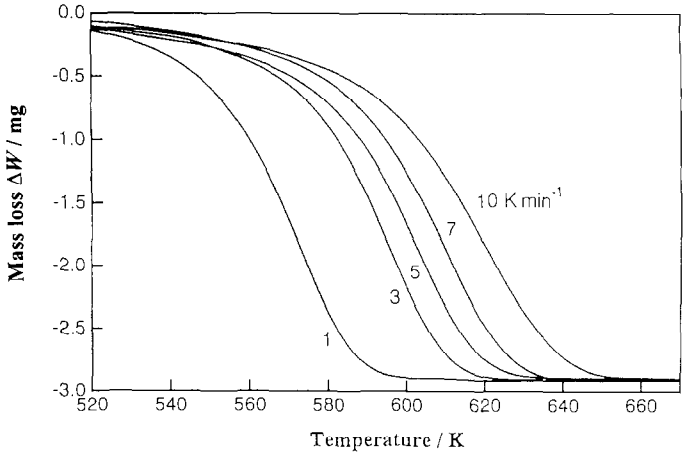


Fig. 3. Typical TG curves for the thermal decomposition of synthetic malachite (10 mg) at different heating rates at a reduced pressure.

plot of $(d\alpha/d\theta)$ versus $M(1-\alpha)[-\ln(1-\alpha)^{1-1/M}]$ was taken to find the values of $M$ and $A$ [29].

### 3.5. α-Nickel(II) sulfate hexahydrate α-$NiSO_4 \cdot 6H_2O$ [30,31]

Fig. 4a shows typical simultaneous TG-DTG curves for the non-isothermal dehydration of single crystals of the hexahydrate [30]. The process is roughly composed of three stages which proceed via the tetrahydrate and monohydrate to the anhydrous product. The reaction behavior is largely affected by the formation of the specific surface product layer at the early stage of non-isothermal dehydration of the hexahydrate. Fig. 5 shows the microscopic evidence of the formation of such a layer. The process of the tetrahydrate to the monohydrate is in particular complicated and is explained on the basis of textural structures produced in the previous step. On the other hand, as shown in Fig. 4b, the dehydration behavior of the crushed crystals is very different from that of the single crystal material.

The non-isothermal dehydration process of crushed crystals of $NiSO_4 \cdot 6H_2O$ is composed of three distinguished dehydration steps, which yields the anhydride via the tetra- and monohydrates [31].The first step of the reaction is surface nucleation of the tetrahydrate, followed by formation of the specific surface product layer of the dihydrate, which influences the advancement of the reaction interface of the hexahydrate-tetrahydrate and diffusion of the evolved water. Kinetic analysis of the first step of the reaction by use of the Expanded Friedman method revealed that the $E$ values change with $\alpha$, indicating complicated kinetic behavior, as expected from the production of the tetra- and dihydrate. Plots of $d\alpha/d\theta$ versus ten possible $f(\alpha)$ showed that the first step of the reaction is best described by the $R_2$ law and the preexponential factor $A$ was found to be 22.5 M $s^{-1}$. Fig. 6 shows the plot of $d\alpha/d\theta$ versus the $R_2$ function. The $R_2$ law was verified by microscopic observation of a thin section of the partly dehydrated materials. The second step includes

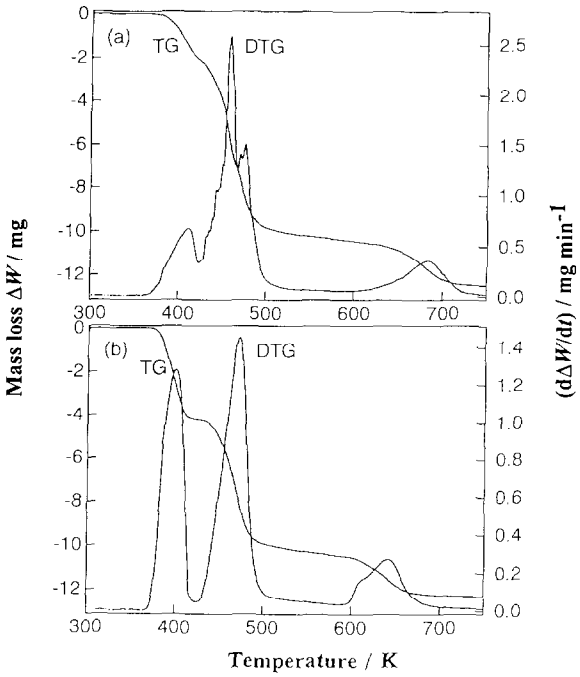


Fig. 4. Typical TG-DTG curves for non-isothermal dehydration of $\alpha$-$NiSO_4 \cdot 6H_2O$. (a) Single crystal: heating rate 10 K $min^{-1}$, atmosphere $N_2$ flow at a rate of 30 ml $min^{-1}$. (b) Crushed crystals: heating rate 8 K $min^{-1}$, atmosphere static air, particle size fraction −32 + 48 mesh.

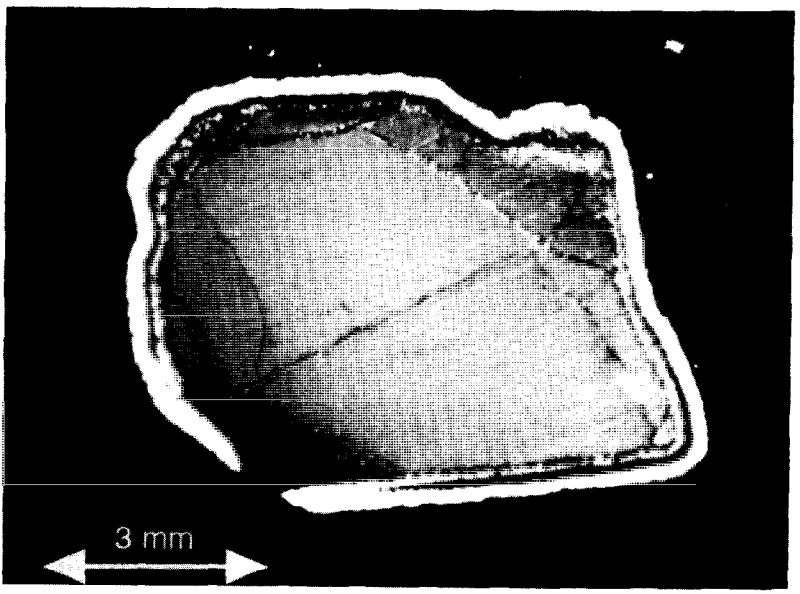


Fig. 5. A typical microscopic view of the thin section of partially dehydrated $\alpha$-$NiSO_4 \cdot 6H_2O$.

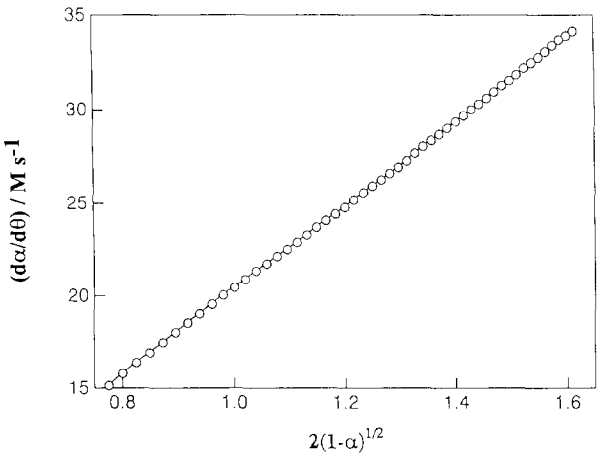


Fig. 6. A plot of $d\alpha/d\theta$ versus $2(1-\alpha)^{1/2}$ for the first step of the non-isothermal dehydration $\alpha$-$NiSO_4 \cdot 6H_2O$.

crack formation which acts as channels for diffusion of the water vapor evolved in the subsequent internal reactions. The reaction behavior of the third step varies with the heating rate, which is related to variation in the morphology and geometry of the intermediate monohydrate.

Under isothermal conditions, the hexahydrate is dehydrated to the dihydrate in which the process consists of surface nucleation of the dihydrate and growth of the nuclei, followed by the advancement of the resultant reaction interface inwards. The significance of the interpretation of the kinetics and mechanism of the solid state decompositions was exemplified by a comparative study of the two characteristic dehydration behaviors under isothermal and non-isothermal conditions.

## 4. The present and future of TA kinetics

Although there are a variety of methods of kinetic analysis of solid state reactions, the same kinetic result might be obtained, from whatever methods of analysis, in principle for a given TA curve recorded. It must be admitted, however, that the kinetic parameters determined from different methods are usually different. This is because of adoption of an inappropriate kinetic model function, analysis beyond the prerequisite introduced in the method, any distortion or deviation in the actual process from the idealized model, along with the experimental errors in TA measurements [32]. For example, it has been pointed out that fluctuation of temperature in the matrix due to self-cooling or self-heating or non-linearity in the linear heating methods poses some problems in obtaining reliable kinetic parameters [25,33]. It is noted here that the Expanded Friedman method is applicable to a system in which the temperature rise is not necessarily linear [13]. Another problem is the change in partial pressure of the evolved gas at the reaction front during the reaction. This is closely connected with the nature of the solid product layer, as well as the thickness of the layer, because of any change in the rate of diffusion of the

gas evolved at the reaction front. It must be borne in mind that the partial pressure inside the matrix cannot, in a strict sense, be specified in the conventional TA measurement, even if the atmosphere outside the matrix is controlled and monitored. In this respect, the controlled transformation rate thermal analysis (CRTA) in which the temperature is so changed that the reaction rate is kept constant during the reaction has an advantage over conventional TA [32,34]. This is because in the case of CRTA the atmosphere around the sample is kept nearly constant during the reaction in which the gaseous product is evolved, compared with conventional TA.

Because TA measurements give only the macroscopically averaged information about the process under investigation, changes in both the experimental and physicochemical factors influencing the kinetics of the process are detected as a change in the position and shape of the TA curves [15,25]. Such a change in the TA curves is projected to the KCE through the mathematical relationships [25,27]. It seems that the establishment of the KCE itself has no physical significance in formulating the kinetics of solid state reactions. It must be admitted that the experimentally resolved shape of TA curves does not always provide a satisfactory source of kinetic data. In addition, if any kinetic software is used, it should include a check system of the reliability of the TA curves as a possible kinetic source.

The method of kinetic calculation must be selected based on such an examination of the TA data in the light of limitation of the kinetic method adopted. Comparison of the kinetic parameters determined using various methods for a given reaction provides us less useful information in view of the kinetic consideration.

The isoconversion method of calculating the activation energy $E$ is useful for checking the constancy of $E$ during the course of a reaction. As the mechanism does not change in such a reaction with constant $E$, further kinetic analyses are possible. Using the constant $E$, an appropriate kinetic law and preexponential factor $A$ are determined: $y(\alpha)$ and $z(\alpha)$ functions defined above are useful for such kinetic analyses. In addition, these functions allow us to check the applicability of the conventional kinetic models and to extend these models to the more sophisticated ones [16].

It is desirable that the kinetic results obtained from TA measurements are complemented, whenever possible, by other techniques such as direct observation of the texture of sample, mass spectroscopy and X-ray diffractometry. Direct observation was often made by optical microscopy, polarizing microscopy, or scanning electron microscopy. Lately a new technique, scanning probe microscopy (SPM) has been developed, which will become a powerful tool for examining changes in the texture of samples. For example, scanning tunnelling microscopy (STM), atomic force microscopy (AFM) and so on will be used effectively in characterizing the surfaces of various solid materials. It is also noted that Modulated DSC (MDSC) which was recently developed has the potential usefulness in better understanding of complicated behaviors of solid state reactions. The method and theory of MDSC have been described by Reading [35,36].

It should be mentioned here that, to increase the reliability of the TA kinetics, the kinetics committee of the International Confederation for Thermal Analysis and Calorimetry (ICTAC) has continued efforts since 1985 [37–39]. The committee made a proposal that a kinetic standard should be established for this purpose, because some sort of standard is important in determining the reliability of the TA curves as a source of the kinetic

data. The kinetic standard is to be based on the reaction with a selected sample under strictly restricted sample and measuring conditions. The characteristic points of the kinetic curve and/or the kinetic parameters determined using the most reliable TA techniques are regarded as standard, and the reliability of a TA apparatus for the kinetic evaluation may be estimated by any deviation from the standard value. It is hoped that such a kinetic standard will bring a universality to the kinetic results obtained from TA measurements [25].

Another important factor is the education in thermal analysis kinetics at training courses organized by the relevant societies and at colleges [40]. It seems that there are very few teaching materials available for such experiments on thermoanalytical kinetics. Therefore, it is evident that versatile teaching materials on the kinetics of solid state reactions should be developed to foster the new generation of scientists working in this interesting field.

## Acknowledgements

The author wishes to thank Dr. Takeo Ozawa, President of the Japan Society of Calorimetry and Thermal Analysis, for his stimulating discussions and suggestions. Thanks are also due to Dr. Nobuyoshi Koga for his help in preparing the manuscript.

## References

[1] K. Honda, Sci. Rep. Tohoku Univ., 4 (1915) 97.
[2] T. Kujirai and T. Akahira, Sci. Papers Inst. Phys. Chem. Res. (Tokyo), 2 (1925) 223.
[3] T. Akahira, Sci. Papers Inst. Phys. Chem. Res. (Tokyo), 9 (1928) 165.
[4] T. Akahira, Sci. Papers Inst. Phys. Chem. Res. (Tokyo), Table No. 3 (1929) 181.
[5] C.D. Doyle, J. Appl. Polym. Sci., 5 (1961) 285; Nature, 207 (1965) 290.
[6] T. Ozawa, Thermochim. Acta, 203 (1992) 159.
[7] T. Ozawa, Bull. Chem. Soc. Jpn., 38 (1965) 1881.
[8] J.H. Flynn and L.A. Wall, J. Polymer Sci. Part B, 4 (1966) 323.
[9] T. Ozawa, J. Therm. Anal., 2 (1970) 301.
[10] T. Akahira and T. Sunose, Res. Report Chiba Inst. Technol., No. 16 (1971) 22.
[11] H.E. Kissinger, Anal. Chem., 29 (1957) 1702.
[12] H. Friedman, J. Polym. Sci., Part C, 6 (1964) 183.
[13] T. Ozawa, J. Therm. Anal, 31 (1986) 547.
[14] J. Sestak and G. Berggren, Thermochim. Acta, 3 (1971) 1.
[15] J. Sestak, J. Therm. Anal., 36 (1990) 1997.
[16] N. Koga, J. Malek, J. Sestak and H. Tanaka, Netsu Sokutei (Calorimet. Therm. Anal.), 20 (1993) 210.
[17] N. Koga and H. Tanaka, J. Phys. Chem., 93 (1989) 7793.
[18] N. Koga and H. Tanaka, J. Therm. Anal., 41 (1994) 455.
[19] R. Ozao and M. Ochiai, J. Ceram. Soc. Jpn., 101 (1993) 263.
[20] E.V. Boldyreva, J. Therm. Anal., 38 (1992) 389.
[21] J.M. Criad, J. Malek and A. Ortega, Thermochim. Acta, 147 (1989) 377; J. Malek, Thermochim. Acta, 138 (1989) 337.
[22] H. Tanaka and N. Koga, J. Phys. Chem., 92 (1988) 7023.
[23] A.K. Galwey, N. Koga and H. Tanaka, J. Chem. Soc. Faraday Trans., 86 (1990) 531.
[24] N. Koga and H. Tanaka, Thermochim. Acta, 185 (1991) 135.

[25] H. Tanaka, N. Koga and J. Sestak, Thermochim. Acta, 203 (1992) 203.
[26] N. Koga and H. Tanaka, Solid State Ionics, 44 (1990) 1.
[27] N. Koga, Thermochim. Acta, 244 (1994) 1.
[28] H. Tanaka and M. Yamane, J. Therm. Anal., 38 (1992) 627.
[29] N. Koga and H. Tanaka, Proc. 30th Anniv. Symp. Calorimetry and Thermal Analysis, Osaka, 1994, p 50.
[30] N. Koga and H. Tanaka, J. Therm. Anal., 40 (1993) 1165.
[31] N. Koga and H. Tanaka, J. Phys. Chem., 98 (1994) 10521.
[32] H. Tanaka, Netsu Sokutei (Calorimet. Therm. Anal.), 19 (1992) 32.
[33 H. Tanaka and N. Koga, J. Therm. Anal., 36 (1990) 2601.
[34] J. Rouquerol, J. Therm. Anal., 5 (1973) 203.
[35] M. Reading, Trends Polym. Sci., 8 (1993) 248.
[36] M. Reading, A. Luget and R. Wilson, Thermochim. Acta, 238 (1994) 295.
[37] J.H. Flynn, M.E. Brown and J. Sestak, Thermochim. Acta, 110 (1987) 101.
[38] J.H. Flynn, M.E. Brown, E. Segal and J. Sestak, Thermochim. Acta, 143 (1989) 45.
[39] J.H. Flynn, Thermochim. Acta, 203 (1992) 519.
[40] H. Tanaka, N. Koga and A.K. Galwey, J. Chem. Educ., 72 (1995) 251.